

Characterization of Near-Sun Coronal Mass Ejection Deflection using Coronagraphic Image Sequences

Jenna Lynn Zink, Department of Physics, George Mason University

1 Problem Statement

Coronal Mass Ejections (CMEs) are eruptions from the Sun's lower atmosphere that contain billions of tons of material and possess their own internal magnetic field. Although the initiation mechanism is still debated (Forbes et al. 2006), many of the proposed scenarios evoke magnetic reconnection. This process causes a sudden release of magnetic energy that drives material and magnetic field outwards. CMEs can have speeds ranging from tens to thousands of km/s.

Explosions from the Sun are a daily occurrence, although their properties vary throughout the solar cycle. As a typical width is ~ 50 degrees or less, only a fraction of CMEs will pass by the near Earth environment on their way to the edge of the solar system. When a CME interacts with the Earth, the main effects include damage to satellites, which include Global Positioning Satellites (GPS) and communication satellites. Radiation effects have been seen on astronauts orbiting Earth and performing extra-vehicular activity and even airline passengers can suffer from this radiation. Due to their internal magnetic fields, when a CME interacts with the Earth's magnetic field it can geo-magnetically induce electric currents in power grids on Earth's surface which can lead to massive power outages, such as the event in Quebec, Canada in 1989.

Currently, forecasting of CME trajectories through the solar system is an active research topic. One approach is to extract CME kinematic properties (speed, size, and direction of motion) from coronagraph images (aided by extreme ultraviolet and x-ray images as well), and use numerical modeling to propagate the CME from the outer edge of the coronagraph images to the Earth's orbit. Typical errors between predicted and detected arrivals at Earth using this approach are seven hours or more (Taktakishvili et al. 2010; Millward et al. 2013). Therefore, currently it is not possible to predict with certainty how a CME observed near the Sun with coronagraphic images will travel through space. However, it is important to know as soon as possible after detection near the Sun if and when a CME may impact the near Earth environment, or other locations in the solar system, and the properties of the bubble when it arrives to the target. With so many space weather effects that can occur when CME impacts with Earth, it is necessary to continue to improve space weather forecasting in order to give the most accurate predictions for CME impact, so that agencies of the national government and private industry can take appropriate action for air travel, power grids, military activity, space walks, and satellite launches.

Since the launch of the STEREO mission, there are now multiple "eyes in the sky" imaging the Sun. These multi-viewpoint coronagraph images can allow us to improve our understanding of the path a CME takes through the solar system. Once a

CME erupts, it does not necessarily travel in a ballistic path away from the Sun. It experiences external forces as it interacts with the solar wind and large-scale coronal magnetic field. Some examples include solar wind drag and magnetic pressure gradient force from coronal holes. These forces can cause a CME to be deflected in its path, and this tends to happen when the CME is near to the Sun (at heights below 0.1 Astronomical Unit; AU). Above this height, the magnetic forces that lead to deflection tend to be weaker, and so it is generally assumed that their direction of propagation does not change much beyond 0.1 AU. In this project, we use CCMC resources to analyze the changes in the position from the first coronagraphic image to the last of a set of 19 events. We determine changes in both latitude and longitude, which is only possible using the combined SOHO-STEREO coronagraph set up.

2 Description of CCMC Models and Tools Used

2.1 DONKI

We used the CCMC's Database of Notifications, Knowledge, and Information (DONKI, <https://kauai.ccmc.gsfc.nasa.gov/DONKI/>) to obtain a list of CMEs during the years 2012-2013. Space weather forecasters, scientists, and the general space weather community use the searchable database. It contains many types of space weather activities, such as flares, CMEs, and geomagnetic storms. The content of the database is the result of the NASA Space Weather Research Center (SWRC) team's daily monitoring of the space environment for NASA robotic mission operators. They measure CMEs in real time with available imagery and enter their size, speed, and direction into DONKI.

2.2 StereoCat

We used the CCMC analysis tool, StereoCat, to analyze the propagation paths of CMEs and to determine their speed and size. StereoCat allows the user to select images of the Sun's outer atmosphere collected by three satellites, the Large Angle and Spectrometric Coronagraph (LASCO; Brueckner et al. 1995) aboard the Solar and Heliospheric Observatory (SOHO) and the Sun Earth Connection Coronal and Heliospheric Investigation (SECCHI; Howard et al. 2008) aboard Solar TERrestrial RELations Observatory Ahead and Behind (STEREO-A and STEREO-B). The tool includes both STEREO beacon (real time) and science-quality images. In this work we selected the science-data images. StereoCat pairs images from the different spacecraft in a user-selected cadence. The result is a set of images to conduct a time lapse analysis of a single CME event.

A session in StereoCat begins with choosing start and end times of a specific solar event, then selecting which two out of the three satellite images provide the best perspective of that event (see Figure 2). The best spacecraft to choose is the one in which the CME is propagating in the plane of sky for that spacecraft, so the ideal separation between the spacecraft and the eruption is 90 degrees. On the Measurement page of StereoCat, there are four images: the top two are the start and end images for one satellite selected and the bottom two are for the second satellite. Using the scientific-data images, the process continues by fitting the bubble of the CME into a cone shape with the vertex

of the cone located at the center of the Sun (Xie et al. 2004). Once the bubble has been fitted to this cone in all four images, the results are displayed in the Session page. An example collection of consecutive measured entries can be seen shown in Figure 3. There are also the means and standard deviations of the entire collection. The parameters needed for this study of CME deflection are the half-width, speed, latitude, and longitude.

StereoCat also can be used in Frameseries Mode in which a series of images over a specific range of time are measured that create graphs of latitude, longitude, speed, acceleration, and half-width over time. The CME bubbles are fitted into cones by the user as described above and the points that are selected for each image remain present on all consecutive images for that satellite. The data points begin to fill in a timeline corresponding to the images' times. For the entire series of images, the results show a 3D summary that includes a mean half-width, linear fit speed, mean latitude and longitude.

2.3 iSWA

The iNtegrated Space Weather Analysis System (iSWA) is used in the forecasting process to monitor the entire space environment. It allows all iSWA system data products that are part of different categories, such as solar, heliosphere, magnetosphere, and planetary/spacecraft data systems, to be combined together to create a single layout. It contains many products, called 'cygnets', that can be opened as windows with different views of the Sun. Some of these cygnets are observational data, and others are models. Using iSWA, we look at the specific date and times of the coronal mass ejections and then see at what specific time frames we should use for analysis in StereoCat.

3 Methodology

3.1 Event Selection

The selection criteria we defined are:

1. CMEs with speeds greater than 1000 km/s. These events are the most vital for space weather because they can cause the most significant damage if they are Earth-directed.
2. Isolated event – not overlapping with another CME in the images
3. Each event had to have a minimum of six images per event and use two out of the three satellites, SOHO, STEREO A and B, in order to do a 3D reconstruction.
4. Pairs of images from different spacecraft must also have less than a ten minute time difference, for example, if an image from SOHO occurred at 10:00UTC, we would need to pair it with an image from either STEREO-A or B that occurred in the range from 9:50UTC to 10:10UTC.
5. We wanted to have a range of CME widths and positions, so we did not restrict these parameters.

Using DONKI (described in Section 2.1), we searched Activity Type “Coronal Mass Ejection” and extracted all events that were measured in real time and determined to be 1,000 km/s or faster during years 2012-2013. Of the events returned by DONKI, 19 events met our criteria. These events are listed in Table 1. The first column is the date and time that the event was first observed by the SWRC team. The next four columns are the speed, longitude, latitude, and full width, as determined by the SWRC team in real time. We are in the process of a comparative study of the CME kinematic properties determined by the SWRC and those determined in this study, but we do not report on those results here.

It is important to note that DONKI’s entries are real time space weather analysis, done with STEREO beacon images. In this work, we used science-level images. This provides two major advantages: 1) we have more images to select from, as not all STEREO beacon data is downloaded and so there are usually data gaps in real time, and 2) the STEREO images are crisper, which makes it easier to locate the front and side edges when fitting with the cone tool.

3.2 CME Measurement

For a successful CME measurement, it is necessary to have a bright and prominent bubble of material that will be easy to see and therefore measure. When using StereoCat to measure a CME, the points that we measure are the edges of the bubble and the leading edge of the ejection as it expands outward. For the sequential measurement, we used the end time image of the first measurement as the next start time image to create a full timeline of single measurements. In the sequential measurements, it is crucial to measure the same part of CME from the previous measurement in order to perform a meaningful triangulation and cone fit.

4 Results

Although we have performed an in-depth analysis of the data, here we show two of our main results. It should be emphasized that the CMEs were selected ‘at random’ in the sense that we did not seek events that should have experienced deflection, such as those that originated near a large coronal hole.

4.1 Deflection as a Function of Speed

In Figure 5, the change in the total deflection is shown as a function of the average CME speed during the time of measurements. We found that six events had minor deflection, defined to be a change of five degrees or less. Twelve events had moderate deflection, defined to be a change of between 6-20 degrees. Only event had strong deflection, defined to be a change of 20 degrees or more.

We compared the CME speed to the total deflection to see if CMEs were more likely to be deflected if they were traveling faster (or slower). Although there is a possible correlation of CME speeds greater than 1,400 km/s with deflection rate, we need more data to explore this trend. We also need to expand our tests to include CMEs with

lower speeds, ranging from 500 km/s to 1000km/s because a different correlation may be possible for the slower CMEs.

4.2 Changes in Latitude and Longitude

In Figure 4, the changes in latitude and longitude are shown for each of the 19 events. We found that seven events had minor changes, defined to be changes of 5 degrees or less in each direction (where direction refers to latitude and longitude). Eleven events had moderate changes, defined to be changes of between 6-20 degrees in one or more directions. Finally, one event had strong changes, defined to be changes of 20 degrees or more in one or more directions.

We did not identify any correlation between changes in the two angles, although there is a positive linear correlation for six of the 19 events.

5 Discussion and Conclusions

From the data analysis performed in this study, we found that most events (12 of 19) undergo moderate deflection (6-20 degrees) during their propagation through the SECCHI COR2 and LASCO C3 field of view. Only one event had a total deflection of greater than 20 degrees, which suggests that strong deflection at heights of 0.05-0.1 AU are rare. We need to analyze more events to confirm these results. The deflections we calculated can modify the arrival time and impact in a CME numerical simulation, and so it is important to account for a possible deflection during space weather operational procedures.

A future step is to go back to these events and look at what features were present on the Sun in order to identify a source for the deflection. How many of the events (with all types of deflection from minor to strong) had strong coronal holes nearby? If we can better understand what causes deflections, then we can better predict the paths of the eruptions, which will help significantly to advance the space weather field as well as better prepare the Earth for any possible interactions with these eruptions.

6 Acknowledgements

The analysis was performed by undergraduate Jenna Zink as a part of her participation in GMU's Undergraduate Research Scholar's Program, under the supervision of Dr. Rebekah Evans.

7 References

- Brueckner, G. E. et al. "The Large-Angle Spectroscopic Coronagraph (LASCO)." 1995, Solar Physics, Vol 162
- Forbes, T. et al. "CME Theory and Models." 2006, Space Sci. Rev., 123, 251
- Howard, R. A. et al. "Sun Earth Connection Coronal and Heliospheric Investigation (SECCHI)." 2008, Space Sci. Rev. 136, 67

Millward, G., D. Biesecker, V. Pizzo, and C. A. de Koning (2013), An operational software tool for the analysis of coronagraph images: Determining CME parameters for input into the WSA-Enlil heliospheric model, *Space Weather*, 11, 57–68, doi:10.1002/swe.20024.

Taktakishvili, A., P. MacNeice, and D. Odstrcil (2010), Model uncertainties in predictions of arrival of coronal mass ejections at Earth orbit, *Space Weather*, 8, S06007, doi:10.1029/2009SW000543.

Xie, H., Ofman, L., and Lawrence, G. “Cone model for halo CMEs: Applications to space weather forecasting.” 2004, *J. Geophys. Res.*, Vol 109.

Table 1: Selected Events

DONKI Activity ID*	DONKI Speed (km/s)	DONKI Longitude	DONKI Latitude	DONKI Width
<i>Year 2012 – 9 Events</i>				
01-02T15:12	1152	99	-17	100
01-19T15:10	1020	-21	46	138
01-23T04:00	2211	26	41	124
01-26T05:30	1082	72	60	60
03-04T11:24	1540	-48	25	120
06-14T14:09	1364	-9	-20	100
07-12T16:54	1480	6	-9	150
07-17T14:25	1100	54	-30	90
07-23T02:36	2930	138	-10	160
<i>Year 2013 – 10 Events</i>				
03-23T12:39	1200	168	-30	56
04-21T16:39	1000	100	10	80
05-13T02:54	1200	-94	20	60
05-17T09:24	1400	-40	13	96
06-13T04:09	1253	171	-25	86
07-22T06:24	1000	157	30	140
08-17T19:24	1081	73	-15	82
11-07T10:39	2100	-135	-13	184
12-12T03:54	1060	51	-31	80
12-26T03:40	1600	-134	-31	180

*Listed in Column 1 is the partial DONKI Activity ID, as the ID is the first four digits, in the format YYYY-MM-DD, also Activity IDs end with the letter “Z”

Figure 1

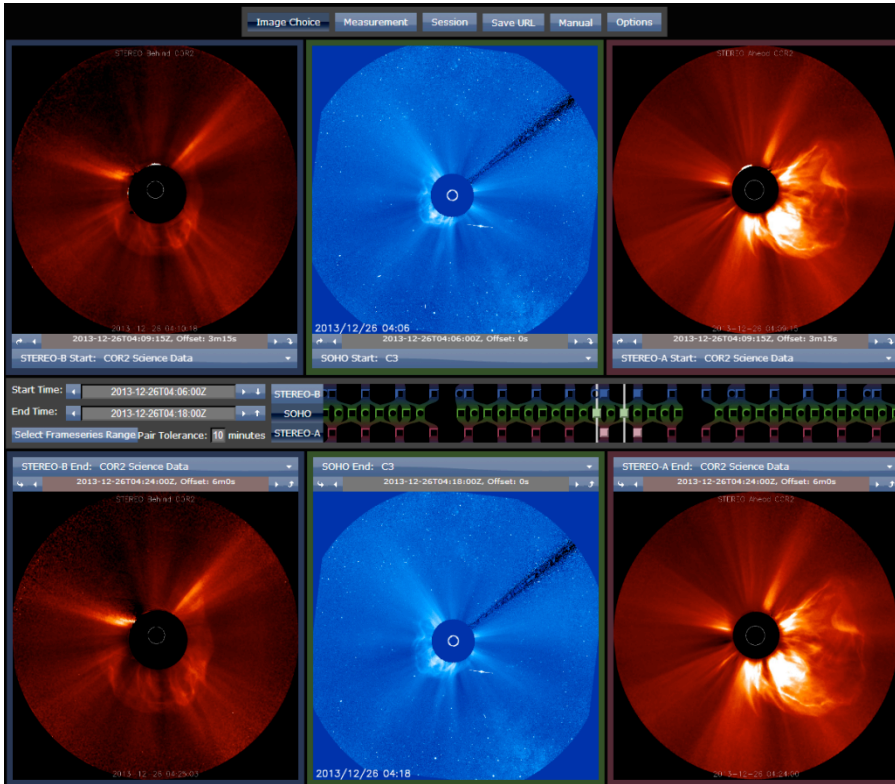


Figure 1: StereoCat's Image Selection page.

Figure 2

Two-Timepoint Measurements										
Projected Measurements						3D Results				
Speed		Half-Width				Half-Width	Speed	Longitude	Latitude	Passes 21.5Rs At
STEREO-B	SOHO	STEREO-A	STEREO-B	SOHO	STEREO-A	Half-Width	Speed	Longitude	Latitude	Passes 21.5Rs At
Free Measurements										
-	708km/s	832km/s	-	66°	51°	57°	849km/s	-132°	-16°	2013-12-26T07:12:13Z
-	997km/s	1399km/s	-	74°	60°	70°	1425km/s	-132°	-21°	2013-12-26T05:41:25Z
-	1066km/s	1496km/s	-	76°	62°	64°	1486km/s	-130°	-24°	2013-12-26T05:37:54Z
-	1243km/s	1496km/s	-	61°	62°	61°	1426km/s	-122°	-23°	2013-12-26T05:44:33Z
-	1093km/s	1518km/s	-	68°	67°	68°	1501km/s	-126°	-22°	2013-12-26T05:36:59Z
-	975km/s	1281km/s	-	75°	69°	74°	1205km/s	-119°	-24°	2013-12-26T06:01:50Z
Means										
-	1014km/s	1337km/s	-	70°	62°	66°	1315km/s	-127°	-22°	2013-12-26T05:59:09Z
Standard Deviations										
-	162km/s	240km/s	-	5°	6°	6°	230km/s	5°	3°	33m42s
Frameseries										
Start Time	End Time	Pairs	Frames Used Per Spacecraft			3D Results Summary				
			STEREO-B	SOHO	STEREO-A	Mean Half-Width	Linear Fit Speed	Mean Longitude	Mean Latitude	Linear Fit Boundary Time
2013-12-26T03:42:00Z	2013-12-26T04:30:00Z	5	-	5/9	3/3	62°	1453km/s	-121°	-25°	2013-12-26T05:40:25Z

Figure 2: StereoCat's Session page that provides the data from the measurements.

Figure 3

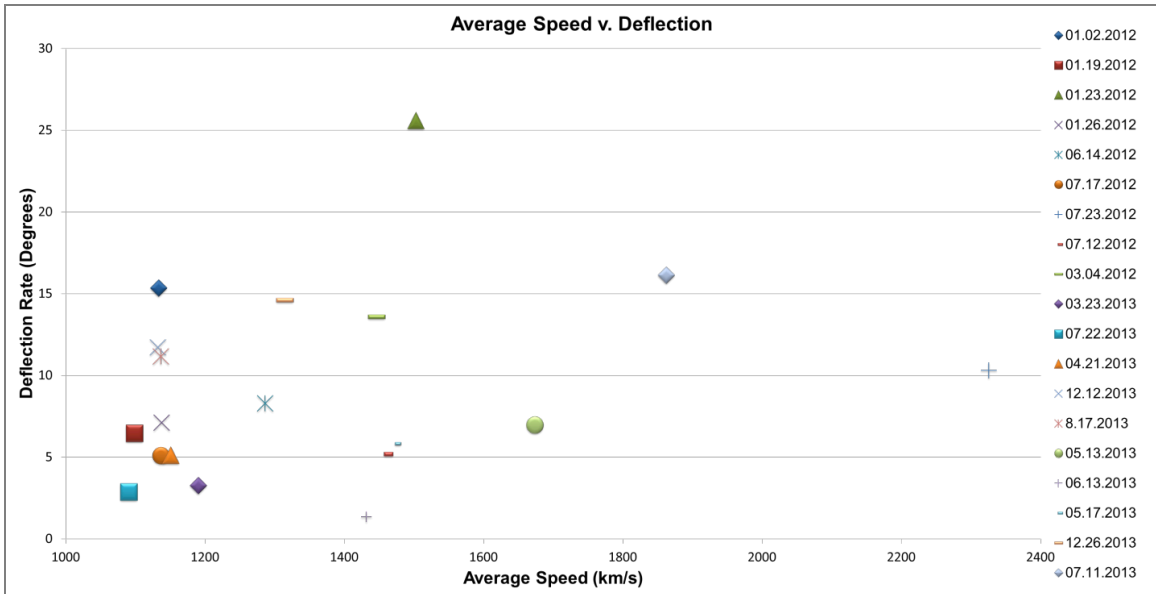


Figure 3: The Total Deflection and the Average Speed. A change is defined as a difference between the measurement in first and last coronagraph image pairs, and e average is the average between the first and last measurements. Due to availability of overlapping images between the different spacecraft, the height of the first and last measurements varies between events.

Figure 4

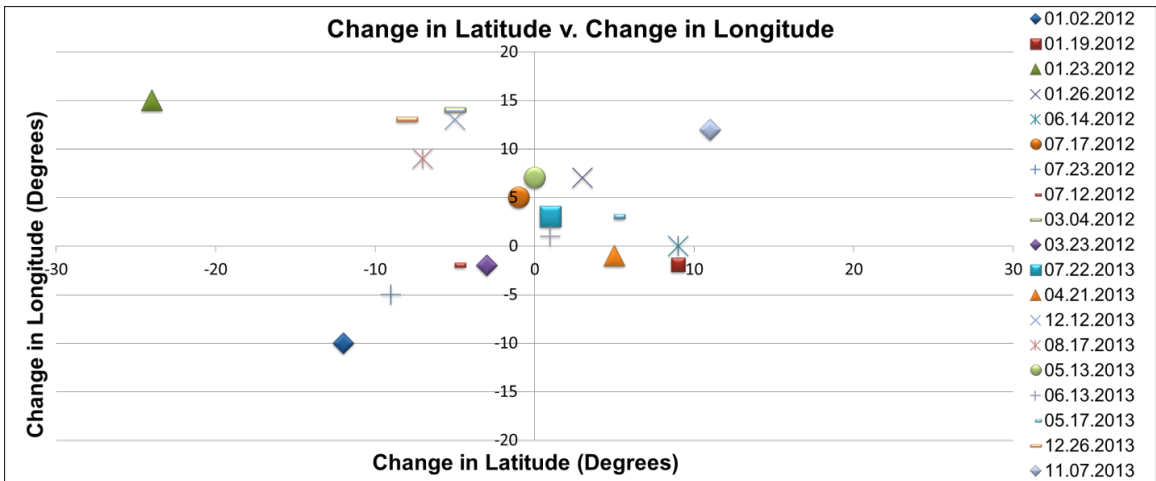


Figure 4: The Change in Latitude and the Change in Longitude. Changes are defined as a difference between the measurement in first and last coronagraph image pairs. Due to availability of overlapping images between the different spacecraft, the height of the first and last measurements varies between events.